Chapter 17
Neural Network Control of a Laboratory Magnetic Levitator

J. Katende
Botswana International University of Science and Technology, Botswana

M. Mustapha
Bayero University, Nigeria

ABSTRACT

Magnetic levitation (maglev) systems are nowadays employed in applications ranging from non-contact bearings and vibration isolation of sensitive machinery to high-speed passenger trains. In this chapter a mathematical model of a laboratory maglev system was derived using the Lagrangian approach. A linear pole-placement controller was designed on the basis of specifications on peak overshoot and settling time. A 3-layer feed-forward Artificial Neural Network (ANN) controller comprising 3-input nodes, a 5-neuron hidden layer, and 1-neuron output layer was trained using the linear state feedback controller with a random reference signal. Simulations to investigate the robustness of the ANN control scheme with respect to parameter variations, reference step input magnitude variations, and sinusoidal input tracking were carried out using SIMULINK. The obtained simulation results show that the ANN controller is robust with respect to good positioning accuracy.

1. INTRODUCTION

Essentially magnetic levitation (maglev) is the use of controlled magnetic fields (or magnetic forces) to cause a magnetic object to float in air in defiance of gravity (Richard, 2004). Maglev systems are widely used in various fields, such as magnetic (non-contact) bearings (Hassan & Mohamed, 2001), high-speed maglev passenger trains (Murai & Tanaka, 2000) and vibration isolation of sensitive machinery (Shen, 2002). Most of the current maglev systems are of the electromagnetic suspension (EMS) type, whereby electric current variations control the attractive force of an electromagnet. The mathematical models of such systems are highly nonlinear and open-loop unstable (Yang, Miyazaki, Kanae & Wada, 2005). Hence it is not a trivial task to construct a high performance controller to accurately position the levitated object.

In recent years, many techniques have been reported in the technical literature for controlling maglev systems. Barrie and Chiasson (1996) as well as Joo and Seo (1997) employed feedback

DOI: 10.4018/978-1-4666-2208-1.ch017

where

$$\left\{\begin{array}{l} A = \begin{bmatrix} 0 & 1 & 0 \\ \dfrac{2Cx_{30}^2}{Mx_{10}^3} & 0 & -\dfrac{2Cx_{30}}{Mx_{10}^2} \\ 0 & \dfrac{2Cx_{30}}{L_1 x_{10}^2} & -\dfrac{R}{L_1} \end{bmatrix} \\ B = \begin{bmatrix} 0 \\ 0 \\ \dfrac{1}{L_1} \end{bmatrix}, C = \begin{bmatrix} 1 & 0 & 0 \end{bmatrix} \end{array}\right. \tag{24}$$

From (24) the linear state space model of the maglev system is

$$\begin{aligned} \dot{x}_1 &= x_2, \\ \dot{x}_2 &= \frac{2Cx_{30}^2}{Mx_{10}^3} x_1 - \frac{2Cx_{30}}{Mx_{10}^2} x_3, \\ \dot{x}_3 &= \frac{2Cx_{30}}{L_1 x_{10}^2} x_2 - \frac{R}{L_1} x_3 + \frac{V}{L_1}. \end{aligned} \tag{25}$$

Figure 3 shows the SIMULINK model of the maglev system represented by the state space model in Equation (25). Figure 4 shows an encapsulation of the SIMULINK model into a single block that is set up using a mask. The mask makes it possible to change the values of M, R, L_1, x_{10}, x_{30} and C for different simulations.

Figure 3. SIMULINK model of the magnetic levitation system

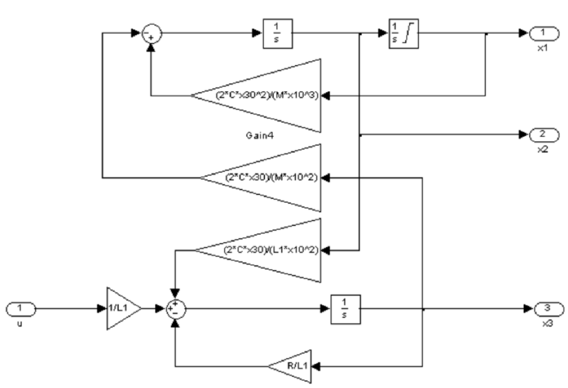

Figure 4. SIMULINK block of the magnetic levitation system

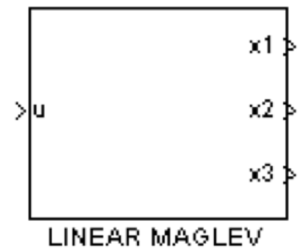

The desired system performance is prescribed by the poles of the general second order system transfer function given in parametric form as (Ogata, 2002)

$$G(s) = \frac{\omega_n^2}{s^2 + 2\zeta\omega_n s + \omega_n^2} \tag{26}$$

The maglev system's closed loop poles are to be placed at $s = p_i (i = 1, 2, 3)$, where p_1 and p_2 are the dominant poles which are determined based on the given specifications in terms of the parameters of Equation (26).

From the specification on peak overshoot, the damping ratio ζ may be computed using (Ogata, 2002):

Peak overshoot

$$M = e^{-\zeta\pi/\sqrt{1-\zeta^2}} x100\% = 5\% \tag{27}$$

$$\Rightarrow \frac{5}{100} = e^{-\zeta\pi/\sqrt{1-\zeta^2}} = 0.05$$

From which the value of ζ can be calculated as $\zeta = \sqrt{\dfrac{8.9744}{\pi^2 + 8.9744}} = \sqrt{0.4762} = 0.6901$

$$\frac{\partial F}{\partial i} = Ri \tag{12}$$

Substituting (9) and (10) in (7) yields

$$M\ddot{y} - Mg + \frac{C}{y^2} i^2 = 0 \tag{13}$$

$$\ddot{y} = g - \frac{C}{M}\left(\frac{i^2}{y^2}\right) = 0 \tag{14}$$

Substituting (11) and (12) in (8) yields

$$\frac{d}{dt}\left(L_1 i + \frac{2C}{y} i\right) + Ri = V \tag{15}$$

$$L_1 \frac{di}{dt} + \frac{2Cy\frac{di}{dt} - 2Ci\dot{y}}{y^2} + Ri = V \tag{16}$$

$$L_1 \frac{di}{dt} + \frac{2C\frac{di}{dt}}{y} - \frac{2Ci\dot{y}}{y^2} + Ri = V \tag{17}$$

$$\left(L_1 + \frac{2C}{y}\right)\frac{di}{dt} - \frac{2Ci\dot{y}}{y^2} + Ri = V \tag{18}$$

It was experimentally found that L_1 is more than 25 times greater than $\frac{L_0 y_0}{y} = \frac{2C}{y}$ [8]. Therefore, by neglecting the term $\frac{2C}{y}$, Equation (18) becomes

$$L_1 \frac{di}{dt} - \frac{2Ci\dot{y}}{y^2} + Ri = V \tag{19}$$

$$\frac{di}{dt} = \frac{2C}{L_1}\left(\frac{i\dot{y}}{y^2}\right) - \frac{R}{L_1} i + \frac{V}{L_1} \tag{20}$$

Let the state variables be chosen such that $x_1 = y, x_2 = \dot{y}, x_3 = i$. Thus substituting these in (14) and (20), the state space model of the magnetic levitation system can be written as

$$\begin{aligned} \dot{x}_1 &= x_2 \\ \dot{x}_2 &= g - \frac{C}{M}\left(\frac{x_3}{x_1}\right)^2 = 0 \\ \dot{x}_3 &= \frac{2C}{L_1}\left(\frac{x_2 x_3}{x_1{}^2}\right) - \frac{R}{L_1} x_3 + \frac{V}{L_1} \end{aligned} \tag{21}$$

3. LINEAR STATE FEEDBACK CONTROLLER DESIGN

The objective is to design a state feedback controller such that the system works according to the following specifications:

- Peak overshoot of approximately 5%.
- Settling time of less than 1 second.

Equations (21) were used to model the open loop maglev system. However, for the design of the linear state feedback controller, the linearized model is required. Using the Jacobian linearization (Katende, 2004), the linear approximation to Equation (21) about the equilibrium point $x_0 = \left[x_{10}, x_{20}, x_{30}\right] = \left[y_0, 0, i_0\right], \quad u_0 = \left[0, 0, V\right]$ is given by

$$\delta\dot{x} = A\delta x + B\delta u \tag{22}$$

$$y = C\delta x. \tag{23}$$

Figure 2. Schematic diagram of a magnetic levitation system

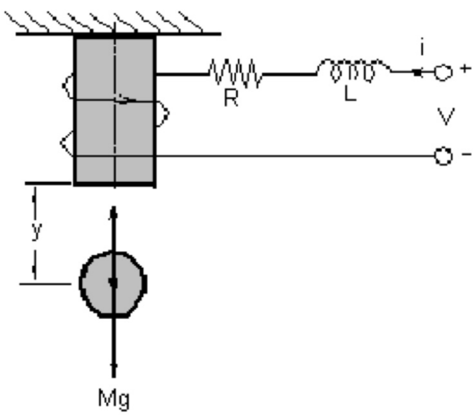

coil; i is current (A) through the coil; R is the coil resistance (Ω); L is the coil inductance (H).

The Lagrange formulation uses the kinetic and potential energies in the system to determine the dynamical equations of motion (Boldia & Nasar, 1986). The kinetic energy of the system (T) is the sum of the kinetic energy of the levitated ball and that of the inductance of the coil and is given by:

$$T = \frac{1}{2} M\dot{y}^2 + \frac{1}{2} L\left(y\right) i^2 \tag{1}$$

The potential energy (P) of the system is given by:

$$P = -Mgy \tag{2}$$

The Rayleigh dissipation function is given by:

$$F = \frac{1}{2} R i^2 \tag{3}$$

The Lagrange function (Γ) is the difference between the kinetic and the potential energies of the system:

$$\Gamma = T - P = \frac{1}{2} M\dot{y}^2 + \frac{1}{2} L\left(y\right) i^2 + Mgy \tag{4}$$

The inductance $L\left(y\right)$ is a nonlinear function of the ball's position, $y,$ that is [8]:

$$L(y) = L_1 + \frac{L_0 y_0}{y} = L_1 + \frac{2C}{y} \tag{5}$$

where y_0 is an arbitrary reference position for the inductance, L_1 is the coil inductance in the absence of the ball, L_0 is additional inductance due to the levitated ball and C is the force constant.

Substituting (5) in (4) yields

$$\Gamma = \frac{1}{2} M\dot{y}^2 + \frac{1}{2}\left(L_1 + \frac{2C}{y}\right) i^2 + Mgy \tag{6}$$

The Lagrangian equations are given by

$$\frac{d}{dt}\left(\frac{\partial \Gamma}{\partial \dot{y}}\right) - \frac{\partial \Gamma}{\partial y} = 0 \tag{7}$$

$$\frac{d}{dt}\left(\frac{\partial \Gamma}{\partial i}\right) + \frac{\partial F}{\partial i} = V \tag{8}$$

The partial derivatives from (6) are,

$$\frac{\partial \Gamma}{\partial \dot{y}} = M\dot{y} \tag{9}$$

$$\frac{\partial \Gamma}{\partial y} = Mg - \frac{C}{y^2} i^2 \tag{10}$$

$$\frac{\partial \Gamma}{\partial i} = \left(L_1 + \frac{2C}{y^2}\right) i \tag{11}$$

linearization techniques to design control laws for maglev systems. Al-Muthairi and Zbiri (2004) and Phuah, Lu and Yahagi (2005) applied the nonlinear sliding mode control technique to improve the positioning accuracy of maglev systems. Other types of controllers for maglev systems reported in the technical literature include: phase-lead compensation (Wong, 1986; Sani, 2004); fuzzy logic controllers (Golob, 2000; Tzes, Chen, & Peng, 1994) and artificial neural network controllers (Kemal, 2003).

Artificial neural networks (ANNs) have shown a great promise in identification and control of nonlinear systems. ANNs constitute a powerful data-modelling tool that is able to capture and represent complex input/output relationships. The motivation for the development of ANN technology stemmed from the desire to develop an artificial system that could perform "intelligent" tasks similar to those performed by the human brain (Hagan, M., Demuth, H., & De Jesus, 2002). ANNs are composed of simple elements operating in parallel. These elements were inspired by biological nervous systems. One can train a neural network to perform a particular function by adjusting the values of the connections (weights) between elements. ANNs have been trained to perform complex functions in various fields of application including pattern recognition, identification, classification, vision and automatic control.

This work considers a laboratory maglev system that was implemented by Sani (2004) and controlled using a lead compensator. An artificial neural network controller for the system is proposed and simulated in the MATLAB/SIMULINK environment. The proposed controller is trained based on the performance of a linear state feedback controller, which was designed to satisfy a pair of dominant poles in the state-space. The rest of the chapter is organized as follows. Section 2 deals with the mathematical modelling of the maglev system. In Section 3 a linear state feedback controller for the maglev system is designed based on well-known engineering specifications of peak overshoot and settling time. Section 4 contains the design and training of an ANN controller for the maglev system. Section 5 presents and discusses simulation results of the proposed ANN controller. Conclusions drawn from the study are given in the last section.

2. MATHEMATICAL MODEL OF THE MAGLEV SYSTEM

The maglev system considered in this paper consists of ferromagnetic ball suspended in a magnetic field. Only the vertical motion is considered. The objective is to keep the ball at a prescribed reference level. The dynamical equations of the maglev system are derived using the Lagrange method.

Figure 1 shows a photograph of the maglev system while Figure 2 shows the corresponding schematic diagram, where: M is the levitated ball mass (kg); g is acceleration due to gravity (m/s^2); V is the voltage (V) applied to the electromagnet

Figure 1. Photograph of a laboratory magnetic levitation system

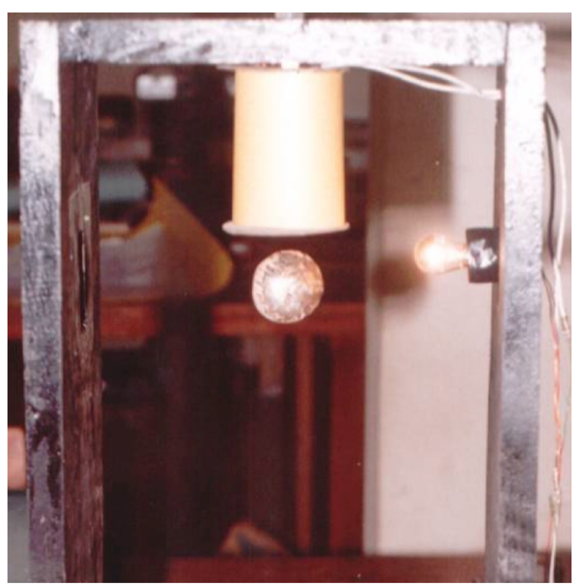

From the specification on settling time, the un-damped natural frequency ω_n may be computed using (23)

$$t_s = \frac{4}{\zeta\omega_n} = 1 \tag{28}$$

Substituting the value of $\zeta = 0.6901$ in Equation (28) and solving for ω_n gives

$$\omega_n = \frac{4}{0.6901*1} = 5.7963$$

Substituting $\omega_n = 5.7963$ and $\zeta = 0.6901$ in (26) gives

$$G(s) = \frac{33.60}{s^2 + 8s + 33.60} \tag{29}$$

Thus the required dominant poles are $p_1 =$ -4.0000 + j4.1952, and $p_2 =$ -4.0000 - j4.1952. The remaining pole is to be located far to the left of the dominant pole-pair and is given as $p_3 = -40$. The state feedback control law is:

$$u = \boldsymbol{K}x + \boldsymbol{N}r \tag{30}$$

where r is the reference command signal. State feedback controller matrix K assigns the closed loop poles while N is a scalar to eliminate off-set between the actual output and the desired output.

Based on the prescribed set of poles the MATLAB pole placement function acker is used to

Box 1.

```
% Matlab code for determining the controller matrix K and scale factor N
I=0.5; L=0.0425; R=3; m= 0.02312; Y=0.01; C=9.07*10^-5;
A=[0 1 0;(2*C*I^2)/(m*Y^3) 0 -(2*C*I)/(m*Y^2);0 (2*C*I)/(L*Y^2) -R/L];
B=[0;0;1/L];
C=[1 0 0];
D=[0];
M=5;                                   % Input desired percent overshoot.
Ts=1;                                  % Input desired settling time.
zeta=(-log(M/100))/(sqrt(pi^2+log(M/100)^2));
                                       % Calculate required damping ratio.
wn=4/(zeta*Ts);                        % Calculate required natural
                                       % frequency.
[num,den]=ord2(wn,zeta);               % Produce a second-order system that
                                       % meets the transient requirements.
r=roots(den);                          % Use denominator to specify dominant
                                       % poles.
poles=[r(1) r(2) -40];                 % Specify pole placement for all
                                       % poles.
K=acker(A,B,poles)                     % Calculate controller gains.
Anew=A-B*K;                            % Form compensated A matrix.
N=-inv(C*inv(Anew)*B)                  % Calculate the scale factor
Bnew=B*N;                              % Form compensated B matrix.
Cnew=C;                                % Form compensated C matrix.
Dnew=D;                                % Form compensated D matrix.
```

compute the controller matrix K. The MATLAB code in Box 1 determines the controller matrix K and the scale factor N.

Running this MATLAB code gives the state feedback controller matrix K and input scale factor N as

$$K = [-103.4559\ -1.6011\ -0.9600] \tag{31}$$

$$N = -1.4559 \tag{32}$$

A SIMULINK model of state feedback controller is developed as shown in Figure 5. The model is encapsulated in a subsystem as shown in Figure 6.

4. NEURAL NETWORK CONTROLLER DESIGN

The ANN structure used in this paper is a 3-layer feed forward network with an input layer, one hidden layer and one output layer as shown in Figure 7.

The input layer, which is not neural, has 3 nodes, the hidden layer has 5 neurons and the output layer has 1 neuron. The activation functions used in the hidden layer and output layer are tansigmoid and pure linear respectively. The network is trained by supervised learning using the pole-assignment state feedback controller as a teacher. The training function uses the Levenberg-Marquardt back-propagation algorithm implemented by the MATLAB function *trainlm*, which updates the ANN weight and bias values (Mathworks, 1998).

For generating the training data a random input, which consists of a series of pulses of random amplitude and duration, is used. Figure 8 shows the SIMULINK model of the maglev system with the pole-assignment state feedback controller for generating the training data. The three controller input signals (x_1, x_2 and x_3) are stored in MATLAB. The target for the neural network is the control signal u generated by the state feedback controller. The three state variables and the control signal are exported to the MATLAB workspace for training the ANN controller.

The MATLAB code in Box 2 trains the neural network.

When the training is finished, the SIMULINK model of the ANN controller is generated using the MATLAB gensim command. The state feedback controller is replaced with the neural network controller as shown in Figure 9.

Figure 5. SIMULINK model of a state feedback controller

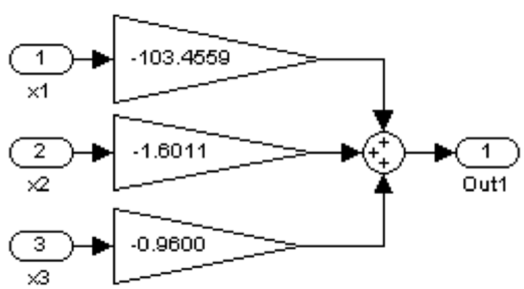

Figure 6. State feedback controller subsystem mask

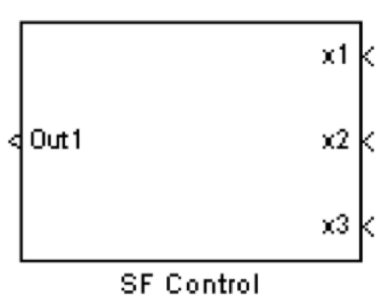

5. SIMULATION RESULTS

Simulation runs were carried out to investigate a number of scenarios. These include:

- Effect of ball mass variations.
- Effect of magnitude of step input command.
- Tracking of sinusoidal reference input.

Figure 7. 3-layer feed forward network

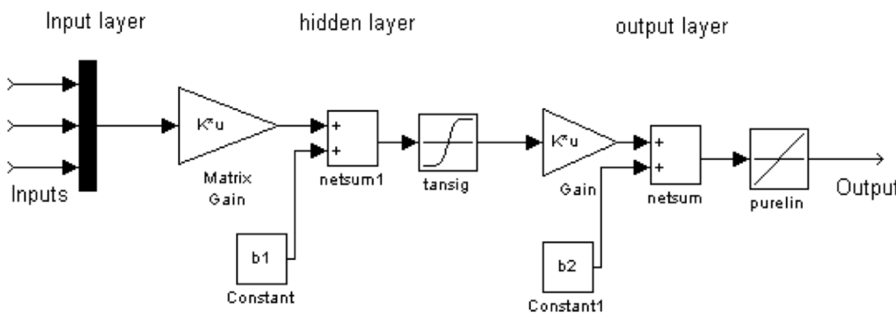

Figure 8. Maglev system for generating the training data

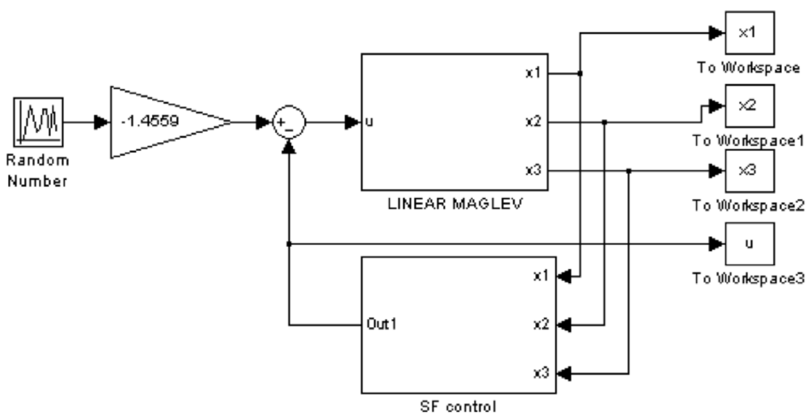

Box 2.

```
% DEFINING THE MODEL PROBLEM
% We would like to train a network to model state feedback
% controller with three inputs and one target output, which
% are exported to matlab workspace after running the
% simulink model of figure 4.

% P is a vector of three input signals.
% newff creates a new feed-forward network with two layers
% (hidden layer with 5 neurons and tansig as the activation
% function, and outpout layer with 1 neuron and purelin as
% the activation function).
% trainlm is the training function

P=[[x1'];[x2'];[x3']];
net=newff([-2 2;-2 2;-2 2],[5,1],{'tansig' 'purelin'},'trainlm');
net.trainParam.epochs=5000; % maximum number of epochs to train
net=train(net,P,u');
```

Figure 9. Maglev system with ANN controller

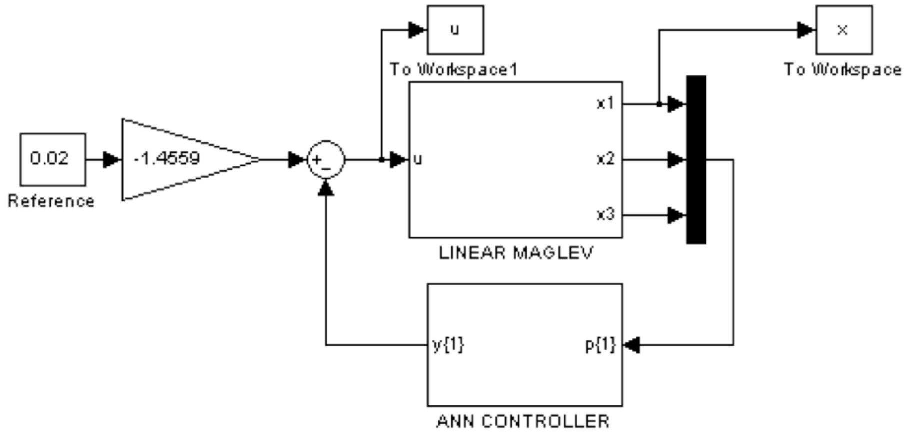

The parameters of the maglev system are as follows [10].

Mass of the ball, M = 0.02312kg,
Coil resistance, R = 3Ω, t
Coil inductance, L_1 = 0.0425H,
Magnetic force constant, C = 9.07x10^{-5}Nm^{2}A^{-2},
Nominal state variables: x_{10} = 0.01m, and x_{30} = 0.5A.

5.1. Ball Mass Variation

To investigate the robustness of the ANN control scheme with respect to parameter variations, simulations were performed with different values of the mass M of the levitated ball commanded to move from the nominal position $y_0 = 0.01m$ to a new position $y = 0.02m$. Thus simulations were performed with the nominal mass M = 0.02312kg, M±25%, and M±50%. Figures 10 and 11 show the plots of ball position versus time. Table 1 summarize the results with respect to peak overshoot, rise time and settling time for the ball position.

From the simulation results, it can be seen that the ball position converges to the commanded value even when the mass of the levitated object varies by ± 50%. Hence, the control system is

Figure 10. Response for M, M+ 25% and M+ 50%

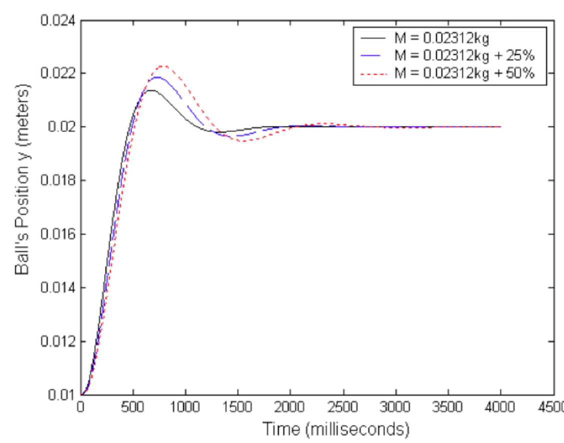

Figure 11. Response for M, M - 25% and M - 50%

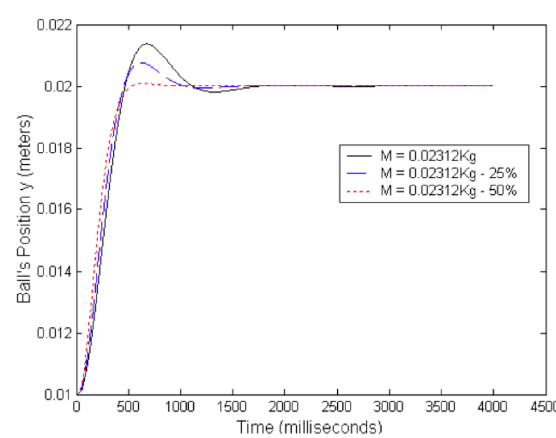

Figure 23. Frequency response of ANN-controlled maglev system

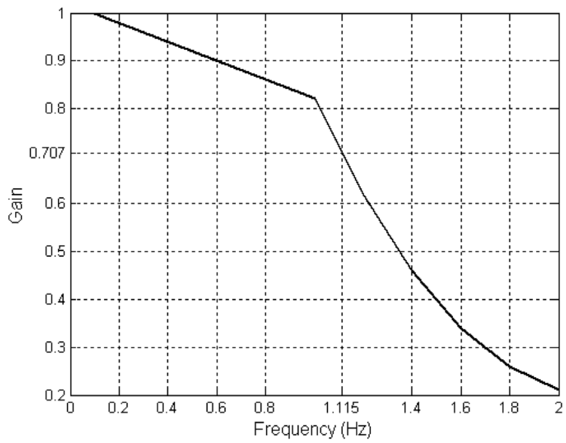

CONCLUSION

In this work, a neural network controller was designed for a laboratory maglev system. The neural network consisted of three layers; the input layer, one hidden layer, and the output layer, with 5 neurons in the hidden layer and 1 neuron in the output layer. The activation functions used in the hidden layer and output layer were *tansig* (hyperbolic tangent sigmoid transfer function) and *purelin* (linear transfer function) respectively. The network was trained by supervised learning using a pole-assignment state feedback controller as a teacher with a random signal as reference. After training a SIMULINK model of the ANN controller was generated.

To evaluate the performance of the ANN controller, simulations were carried using SIMULINK. The ball's mass was varied in the range ± 50% of the nominal value and the step response simulation results showed that, the ball position converges to the desired value even when the mass of the levitated ball varies by ± 50%. It was observed that the peak overshoot decreases if the ball mass is less than the nominal value and increases when the ball mass is greater the nominal value. Moreover, the ANN-controlled system's peak overshoot was higher than the specified 5% even though the desired position was achieved in all simulation scenarios. Thus in terms of positioning accuracy, the ANN is very robust but the dynamic accuracy was found to be inadequate.

The ball's command position was varied in the range 0.002m and 0.3m. The simulation results showed that in all cases the ball position converges to its desired value and there was no change in the peak overshoot, settling time and rise time (i.e. 14%, 0.95s, and 0.3s respectively). The maximum ball's position that the ANN controller can handle was 0.4m.

Simulations were also performed for the maglev system with the ANN controller using sinusoidal reference input of amplitude 0.001m with different frequencies. The simulation results showed that, the ANN controller tracks the sinusoidal reference input in the bandwidth of 1.115Hz. Further work is looking into how to effectively reduce the peak overshoot and practical implementation of the ANN controlled maglev system.

Figure 18. Position for 1.2Hz

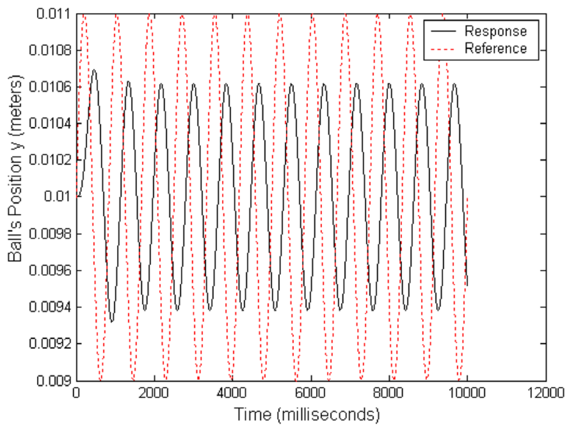

Figure 19. Position for 1.4Hz

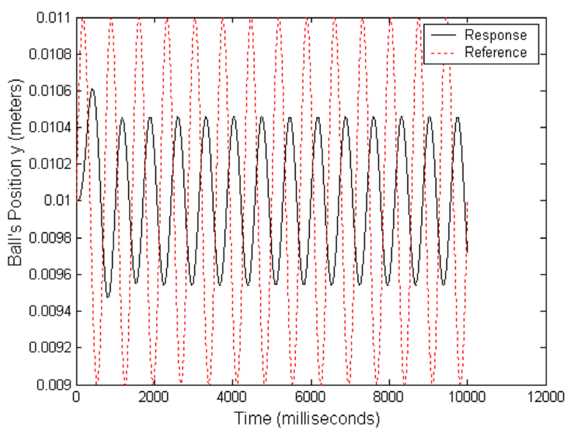

Figure 20. Position for 1.6Hz

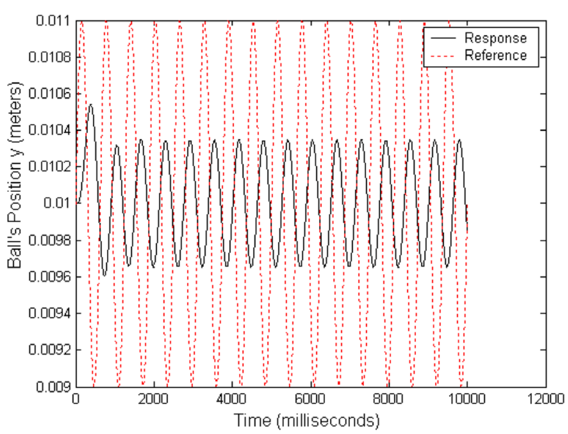

Figure 21. Position for 1.8Hz

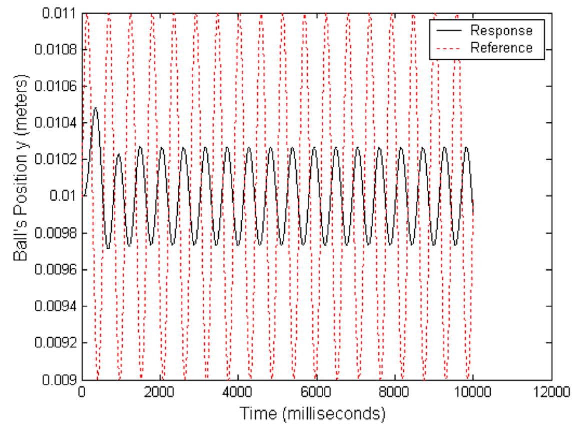

Figure 22. Position for 2Hz

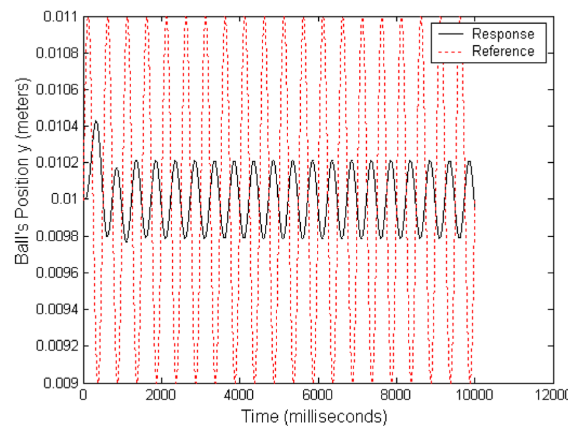

Table 3. Summary of ANN controller simulation results with sinusoidal input for different frequencies

Frequency (Hz)	Amplitude of Response Signal (m)	Gain
0.1	0.00100	1.00
1.0	0.00082	0.82
1.2	0.00062	0.62
1.4	0.00046	0.46
1.6	0.00034	0.34
1.8	0.00026	0.26
2.0	0.00021	0.21

Figure 15. Step response for 0.3m

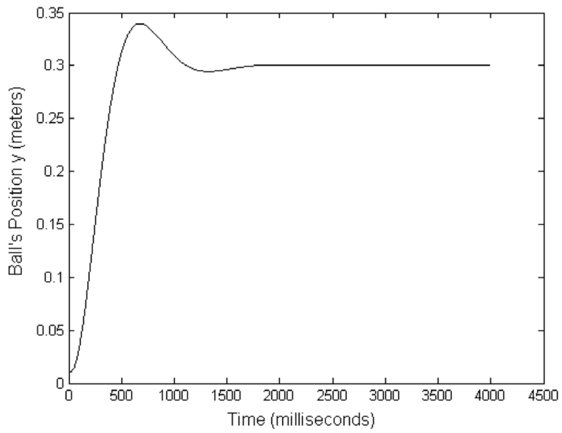

Table 2. Summary of ANN controller simulation results for different ball positions

Ball's Position	Percent Overshoot	Rise Time	Settling Time
0.002m	14%	0.3s	0.95s
0.02m	14%	0.3s	0.95s
0.1m	14%	0.3s	0.95s
0.3m	14%	0.3s	0.95s

5.3. Sinusoidal Input Tracking

Simulations were also performed for the maglev system with the neural network controller using sinusoidal reference input of amplitude 0.001m with different frequencies. The simulations were performed with the frequency of the reference signal set to 0.1Hz, 1Hz, 1.2Hz, 1.4Hz, 1.6Hz, 1.8Hz, and 2Hz, respectively. Figures 16 through 22 show the plots of position versus time. From the simulation results, it can be seen that as the frequency of the input signal increases, the amplitude of the response decreases. Table 3 summarizes the simulation results.

In order to find the bandwidth of the system a graph of gain versus frequency was plotted as shown in Figure 23, using the Matlab code in Box 3.

Box 3.

```
frequency =[0.1 1 1.2 1.4 1.6 1.8 2];
gain =[1 0.82 0.62 0.46 0.34 0.26 0.21];
plot(frequency,gain,'black')
```

Figure 16. Position for 0.1Hz

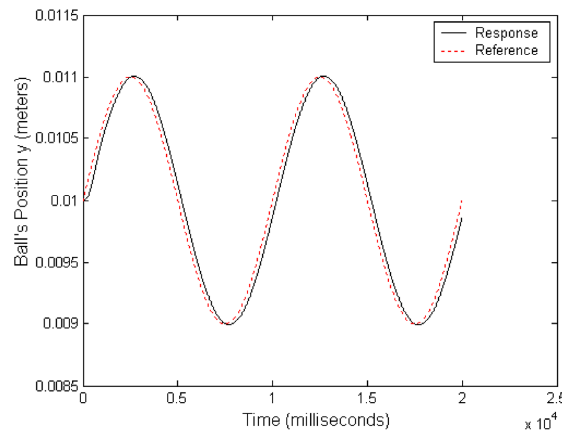

Figure 17. Position for 1Hz

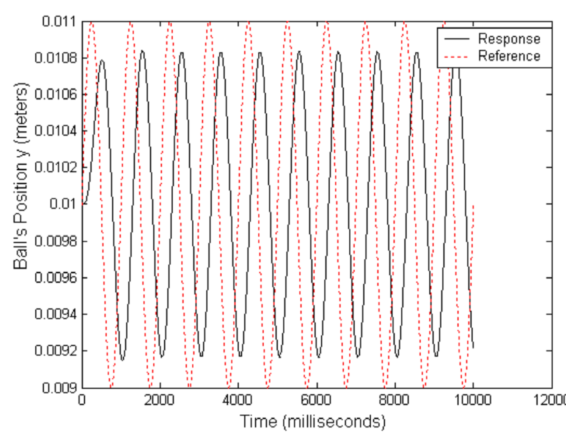

From Figure 23 it can be seen that the bandwidth of the system is 1.115Hz.

Table 1. Summary of ANN controller simulation results for different values of M

Ball Mass	Peak Overshoot	Rise Time	Settling Time
0.02312kg	14%	0.3s	0.95s
0.02312 - 25%	8%	0.29s	0.76s
0.02312 - 50%	1%	0.29s	0.42s
0.02312 + 25%	19%	0.31s	1.06s
0.02312 + 50%	23%	0.34s	1.5s

robust with respect to changes in the ball mass. Also, it can be seen that from the simulation results the percent overshoot and settling time decrease with decrease in mass and increase with the increase in mass. While the rise time increases with increase in mass and remains constant with decrease in mass.

5.2. Effect of Step Input Magnitude

Simulations were also performed for the maglev system with the neural network controller for different positions of the ball. The simulations are performed with the position set to 0.002m, 0.02m, 0.1m and 0.3m respectively. Figures 12 through 15 show the plots of position versus time. Table 2 summarizes the ball's position peak overshoot, rise time and settling time.

From the simulation results, it can be seen that the position converges to any set value within the range 0.002m to 0.3m. Hence, the control system is robust with respect to changes in the step input magnitude. Also, it can be seen that from the simulation results there is no change in peak overshoot, rise time and settling time when the command position is varied.

Figure 12. Step response for 0.002m

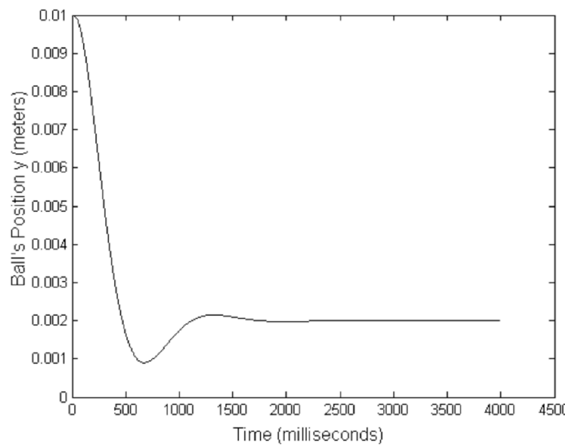

Figure 13. Step response for 0.02m

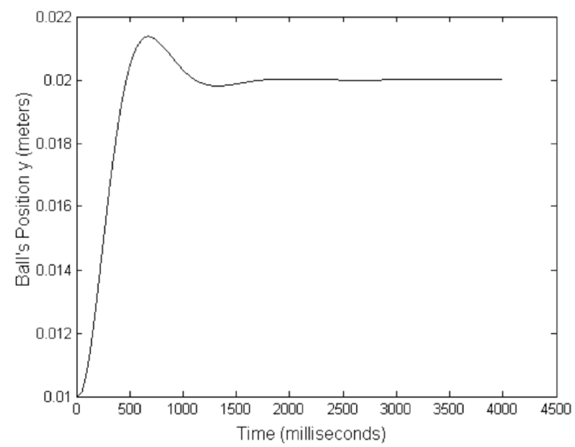

Figure 14. Step response for 0.1m

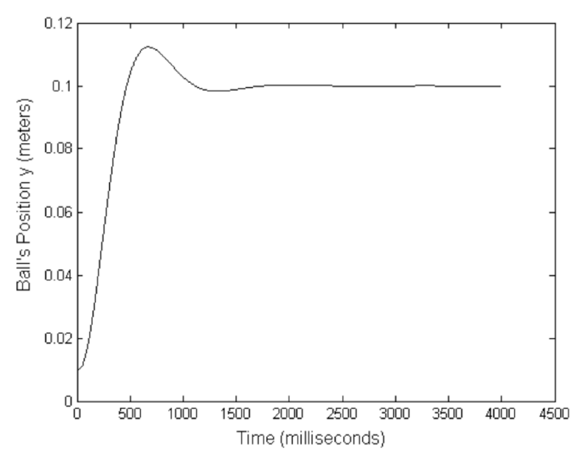

REFERENCES

Al-Muthairi, N. F., & Zbiri, M. (2004). Sliding mode control of a magnetic levitation system. *Mathematical Problems in Engineering*, *2*, 93–107. doi:10.1155/S1024123X04310033.

Barrie, W., & Chiasson, J. (1996). Linear and nonlinear state-space controllers for magnetic levitation. *International Journal of Systems Science*, *27*(11), 1153–1163. doi:10.1080/00207729608929322.

Boldia, I., & Nasar, S. A. (1986). *Electric machines dynamics*. New York: Macmillan.

Demuth & De Jesus, O. (2002). An introduction to the use of neural networks in control systems. *International Journal of Robust and Nonlinear Control*, *12*(11), 959–985. doi:10.1002/rnc.727.

Golob, M. (2000). *Decomposition of a fuzzy controller based on the inference break-up*. (Doctoral Thesis). University of Maribor, Maribor, Slovenia.

Hassan, I. M. M., & Mohamed, A. M. (2001). Variable structured control of a magnetic levitation system. In *Proceedings of the American Control Conference*. Arlington, VA: IEEE Press.

Joo, S., & Seo, J. H. (1997). Design and analysis of the nonlinear feedback linearizing control for an electromagnetic suspension system. *IEEE Transactions on Control Systems Technology*, *5*(1), 135–144. doi:10.1109/87.553672.

Katende, J. (2004). *Linear systems theory*. (Unpublished Master's Thesis). Bayero University, Kano, Nigeria.

Kemal, N. A. (2003). *Control of magnetic suspension system using state feedback, optimal, and neural network controllers*. (Unpublished Master's of Engineering Thesis). Bradley University, Maribor, Slovenia.

Mathworks. (1998). Retrieved from http://www.mathworks.com

Murai, M. & Tanaka, M. (2000). Magnetic levitation (maglev) technologies. *Japan Railway & Transport Review,* (25), 61–67.

Ogata, K. (2002). *Modern control engineering*. New Delhi: Prentice-Hall.

Phuah, J., Lu, J., & Yahagi, T. (2005). *Chattering free sliding mode control in magnetic levitation systems*. Chiba, Japan: Chiba University. doi:10.1541/ieejeiss.125.600.

Richard, C. D. (2004). *Magnetic levitation: A straightforward and fast information guide to magnetic levitation.* Retrieved from www.clearlyexplained.com

Sani, D. S. (2004). *Design and development of a magnetic levitation system*. (Unpublished Master's of Engineering Thesis). Bayero University, Kano, Nigeria.

Shen, J. (2002). H^∞ control and sliding mode control of magnetic levitation system. *Asian Journal of Control*, *4*(3), 333–340. doi:10.1111/j.1934-6093.2002.tb00361.x.

Tzes, A., Chen, J. C., & Peng, P. Y. (1994). Supervisory fuzzy control design for a magnetic suspension system. In *Proceedings of the 30th IEEE Conference on Fuzzy Systems,* (vol. 1, pp. 138-143). IEEE Press.

Wong, T. (1986). Design of a magnetic levitation system. *IEEE Transactions on Education*, *29*, 196–200. doi:10.1109/TE.1986.5570565.

Yang, Z., Miyazaki, K., Kanae, S., & Wada, K. (2004). Robust position control of a magnetic levitation system via dynamic surface control technique. *IEEE Transactions on Industrial Electronics*, *51*(1), 26–34. doi:10.1109/TIE.2003.822095.